Am J Transl Res 2018;10(12):4065-4081
www.ajtr.org /ISSN:1943-8141/AJTR0077292

Original Article

Endothelial cells from different anatomical origin have distinct responses during SNAIL/TGF-β2-mediated endothelial-mesenchymal transition

Mariana Tomazini Pinto[1,2,4], Fernanda Ursoli Ferreira Melo[1], Tathiane Maistro Malta[1], Evandra Strazza Rodrigues[1], Jessica Rodrigues Plaça[1], Wilson Araújo Jr Silva[1,3], Rodrigo Alexandre Panepucci[1,3], Dimas Tadeu Covas[1,3], Claudia de Oliveira Rodrigues[5,6], Simone Kashima[1,2]

[1]National Institute of Science and Technology in Stem Cell and Cell Therapy, Center for Cell-Based Therapy and Regional Blood Center of Ribeirão Preto, Brazil; [2]Faculty of Pharmaceutical Sciences, [3]Faculty of Medicine of Ribeirão Preto, University of São Paulo, Ribeirão Preto, Brazil; [4]Molecular Oncology Research Center, Barretos Cancer Hospital, Barretos, SP, Brazil; [5]Department of Molecular and Cellular Pharmacology, [6]Interdisciplinary Stem Cell Institute, University of Miami Leonard M, Miller School of Medicine, Miami, Florida, USA

Received April 3, 2018; Accepted October 17, 2018; Epub December 15, 2018; Published December 30, 2018

Abstract: Background: Endothelial-mesenchymal transition (EndMT) is a complex process whereby differentiated endothelial cells undergo phenotypic transition to mesenchymal cells. EndMT can be stimulated by several factors and the most common are the transforming growth factor-beta (TGF-β) and SNAIL transcription factor. Given the diversity of the vascular system, it is unclear whether endothelial cells lining different vessels are able to undergo EndMT through the same mechanisms. Here we evaluate the molecular and functional changes that occur in different types of endothelial cells following induction of EndMT by overexpression of SNAIL and TGF-β2. Results: We found that responses to induction by SNAIL are determined by cell origin and marker expression. Human coronary endothelial cells (HCAECs) showed the greatest EndMT responses evidenced by significant reciprocal changes in the expression of mesenchymal and endothelial markers, effects that were potentiated by a combination of SNAIL and TGF-β2. Key molecular events associated with EndMT driven by SNAIL/TGF-β2 involved extracellular-matrix remodeling and inflammation (IL-8, IL-12, IGF-1, and TREM-1 signaling). Notch signaling pathway members DLL4, NOTCH3 and NOTCH4 as well as members of the Wnt signaling pathway FZD2, FZD9, and WNT5B were altered in the combination treatment strategy, implicating Notch and Wnt signaling pathways in the induction process. Conclusion: Our results provide a foundation for understanding the roles of specific signaling pathways in mediating EndMT in endothelial cells from different anatomical origins.

Keywords: Endothelial-mesenchymal transition (EndMT), endothelial cells, SNAIL, transforming growth factor beta 2 (TGF-β2)

Introduction

Endothelial-mesenchymal transition (EndMT) is a phenotypic conversion whereby endothelial cells acquire mesenchymal characteristics. During EndMT, the expression of mesenchymal markers including fibroblast-specific protein 1 (FSP-1), α-smooth muscle actin (α-SMA), collagen, type I, alpha 1 (COL1A1), fibronectin, N-cadherin, and vimentin are enhanced at the expense of endothelial markers such as CD31, vascular endothelial cadherin (VE-cadherin), and von Willebrand factor (vWF) that, are decreased. The resulting in cells acquire the invasive and migratory capacities of mature MSCs [1-5].

EndMT was originally described during heart development where endocardial endothelial cells that line the atrioventricular canal undergo transition to form the endocardial mesenchymal cushion that later gives rise to the septum and mitral and tricuspid valves [6]. Several reports have shown that postnatal EndMT contributes to pathologies including cancer progression [7], cardiac, renal, and pulmonary fibrosis [8-10], and wound healing [11]. Members of the transforming growth factor-beta

(TGF-β) family are potent inducers of EndMT. Although, all three TGF-β isoforms (TGF-β1, TGF-β2 and TGF-β3) have been associated with EndMT induction, TGF-β2 appears to be the most effective activator [12, 13]. Induction of EndMT triggers upregulation of SNAIL, a zinc-finger-containing transcription factor that suppresses the expression of genes encoding proteins involved in the maintenance of adherents and tight junctions [2, 14, 15]. SNAIL is required for TGFβ-induced EndMT and has been found to be highly expressed in endothelial cells associated with many types of cancer [16-18]. One study showed that siRNA-mediated knockdown of SNAIL expression was sufficient to inhibit TGF-β2-induced EndMT in cultured endothelial cells [19].

Although numerous studies have confirmed a critical role for EndMT in heart development and pathology, few studies have examined the molecular changes occurring in endothelial cells during transition and the transcriptional networks that mediate EndMT remain unclear. Because endothelial cells from different vascular beds have distinctive characteristics and gene expression profiles [20, 21], it is not clear whether such endothelial cells from different origins share the same EndMT induction mechanisms. Therefore, the aim of the present study was to evaluate the molecular and functional changes that occur in different types of endothelial cells after induction of EndMT by stimulation of SNAIL and TGF-β2 signaling pathways.

Materials and methods

Cell lines and culture conditions

Human umbilical vein endothelial cells (HUVEC-ATCC® PCS-100-013™), human pulmonary artery endothelial cells (HPAEC-ATCC® PCS-100-022™), human aortic endothelial cells (HAEC-ATCC® PCS-100-011™), and human coronary artery endothelial cells (HCAEC-ATCC® PCS-100-020™), were purchased from American Type Culture Collection (ATCC) and maintained according to manufacturer's instruction in EGM™-2 Endothelial Cell Growth Medium-2 BulletKit (EGM-2 - Lonza). All cells were compared at passage 5 and maintained under 37°C and 5% CO_2 humidified atmosphere. For western blot analysis and migration assays, HCAECs were used between passages 5-8.

SNAIL lentivirus production and endothelial cell transduction

Human embryonic kidney 293FT cells were maintained in DMEM (Gibco) medium supplemented with 10% fetal bovine serum (FBS), 0.1 mM MEM Non-Essential Amino Acids (NEAA), 1% Pen-Strep, and 500 μg/ml Geneticin (complete DMEM medium). 293FT cells were used to generate SNAIL lentiviral vector by co-transfection of plasmid DNA vector pLVX-IRES-ZsGreen (Clontech) carrying SNAIL cDNA and the packaging plasmids pDR 8.91 and pMD2-VSV-G using Lipofectamine® 2000 (Life Technologies). For generation of control lentivirus, cells were packed with empty plasmid vector. Cells were transfected at 80% confluence in complete DMEM medium, according to manufacturer's instructions. After 6 hours of transfection, media was replaced and culture supernatants collected 48 h and 72 h afterwards. The culture supernatants were filtered and used for transduction of endothelial cells.

Induction of EndMT

EndMT was induced by SNAIL overexpression (Treatment I) or a combination of TGF-β2 and SNAIL overexpression (Treatment II). In treatment I, endothelial cells were transduced with a lentiviral vector expressing SNAIL cDNA. The culture supernatants containing viruses were added to the cells in the presence of 6 μg/ml Polybrene (Sigma-Aldrich). Six hours after transduction, the virus-containing media was replaced by EGM-2 medium, and the plate was incubated overnight. Two cycles of transduction were performed. Empty lentiviral vector was used as control. After transduction, cells were maintained for five days in EGM-2 medium without serum. At the end of this period, green fluorescent protein (GFP) positive cells were sorted using a FACSort analyzer (Becton Dickinson) and immediately processed for gene and protein expression analysis. In combined treatment II, endothelial cells were simultaneously transduced with SNAIL overexpressing virus and treated with 10 ng/ml human recombinant TGF-β2 (R&D Systems Inc.) every 24 hours for a total period of 5 days.

RNA isolation and real-time quantitative PCR

Total RNA was isolated with TRIzol Reagent (Invitrogen) and reverse-transcribed by random

priming using a High Capacity cDNA Reverse Transcription Kit (Applied Biosystems) following the manufacturer's instructions. Gene expression analysis was performed by quantitative PCR (qPCR) using with TaqMan® Gene Expression Assays (Applied Biosystems). qPCR amplification was performed with ABI Prism 7500 Sequence Detection System (Applied Biosystems). Control and EndMT-induced samples were analyzed for the expression of SNAIL (*SNAI1*-Hs00195591_m1), fibronectin (FN1-Hs01549976_m1), S100 calcium binding protein A4 (FSP1-Hs00243202_m1), thy-1 cell surface antigen (CD90-Hs00174816_m1); smooth muscle protein 22-alpha (SM22-Hs00162558_m1); calponin (CNN1-Hs00154543_m1); platelet endothelial cell adhesion molecule (CD31-Hs00169777_m1); cadherin 5 (VE-cadherin-Hs00174344_m1); collagen type I alpha 1 (COL1A1-Hs00164004_m1); collagen type I alpha 2 (COL1A2-Hs00164099_m1); NOTCH3 (Hs00166432_m1); NOTCH4 (Hs00270200_m1); catenin beta (CTNNB1-Hs00355045_m1); wingless-type MMTV integration site family (WNT5B). All expression data were normalized to the geometric mean of actin beta (ACTB-4326315E) and glyceraldehyde-3-phosphate dehydrogenase (GAPDH-4310884E). Relative expression was calculated using the 2^{-ddCt} method [22], comparing EndMT-induced versus untreated control samples.

Western blot analysis

After EndMT induction, control and treated cells were harvested in RIPA buffer (Sigma) according to manufacturer's instructions. As a positive control, we also harvested endothelial cells treated with 10 ng/ml human recombinant TGF-β2 (R&D Systems Inc.) every 24 hours for a total period of 5 days. Protein concentration was estimated using BCA™ Protein Assay kit (Thermo Scientific). Equal protein amounts were loaded in a 10% gel (Bio-Rad), separated by SDS-PAGE and transferred to nitrocellulose membrane (Amershan Biosciences). Membranes were blocked in 5% nonfat milk (diluted in Tris-buffered saline and 0.1% Tween-20) for 1 hour at room temperature. Blots were incubated with primary anti-CD31 (Cell Signaling Technology #3528), anti-VE-cadherin (Cell Signaling Technology #2158), anti-SM22 (Abcam-ab14106), anti-SNAIL (Cell Signaling Technology #3895), anti-COL1A1 (Abcam-ab34710), and anti-GAPDH (Cell Signaling Technology #2118) antibodies (1:1000) overnight at 4°C. This procedure was followed by incubation with sheep anti-mouse or anti-rabbit HRP-labeled secondary antibody (1:2000) for 1 hour at room temperature. Immunoreactive bands were visualized using the ImageQuant™ LAS 4000 mini (GE Healthcare Amersham) after exposure to ECL Prime Western Blotting Detection Reagent (GE Healthcare).

Microarray analysis

Gene expression profiling was performed in HCAECs before and after induction of EndMT using One-Color Microarray-Based Gene Expression Analysis (Low Input Quick Amp Labeling) (Agilent Technologies), according to the manufacturer's instructions. Total RNA was isolated and purified with the RNeasyMini Kit (Qiagen). The microarray was scanned with an Agilent Microarray Scanner (Agilent Technologies), and data were processed using Feature Extraction software version 10.7.3 (Agilent Technologies). Quality control and array normalization were done using bioconductor package (http://bioconductor.org/). Differentially expressed genes were identified based on a log10 fold change > 2 and a statistically significant level using P adjusted < 0.005. Ingenuity Pathway Analysis (IPA) was used to evaluate the microarray data for relevant biological themes within the differentially expressed genes. Microarray data have been deposited in the NCBI Gene Expression Omnibus (www.ncbi.nlm.nih.gov/geo/) (GEO ID: GSE96089). Samples analyzed included control cells without any treatment (CT) (n = 2), cells transduced with empty vector (n = 2), transduced with SNAIL virus (n = 3) and cells treated with a combination of SNAIL overexpression and TGF-β2 (SNAIL+TGF-β2) (n = 3).

Migration assays

EndMT was induced as described above. After reaching confluence, the cell monolayer was scratched with a pipette tip and gently washed twice with phosphate-buffered saline (PBS) to remove floating scrapped cells. EGM-2 medium with all supplements provided by manufacture, except serum was added and cells placed back in incubator for 24 hours. Phase contrast micro-

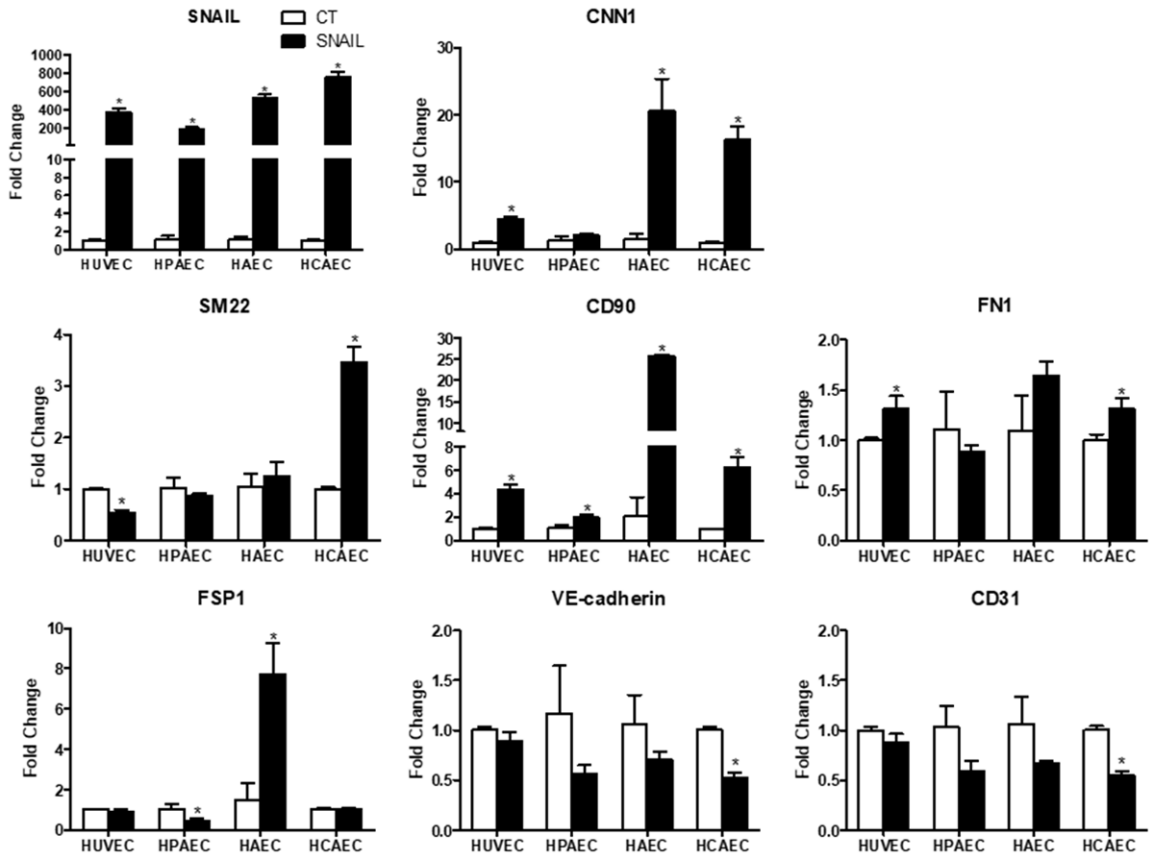

Figure 1. Effect of SNAIL overexpression on EndMT induction in human endothelial cells from different anatomical origins. Expression analysis of endothelial (CD31 and VE-cadherin) and mesenchymal (SNAIL, CNN1, SM22, CD90, FN1, and FSP1) markers in endothelial cells transduced with SNAIL lentivirus (SNAIL) by qPCR. Results are expressed as log fold-changes relative to control (CT) after normalization to at least two endogenous control genes (n = 3-4, *P ≤ 0.05).

graph images were captured immediately after scratching and 24 hours later to determine the ratio of migration. The relative distance traveled by the leading edge was assessed using ImageJ software. The effect of EndMT inducers on cell migration was expressed as percentage of migration relative to day zero, when the scratch was created.

Statistical analysis

Results between individual control and treatment groups were analyzed for significance using t-test. One-Way ANOVA or ANOVA on Ranks (depending on data distribution) were used for comparison of multiple treatment groups, followed by Dunn's or Newman-Keuls multiple comparison post-tests. All statistical tests were performed with Sigma-Plot and GraphPad Prism Software. Differences were considered statistically significant when *p* values were $P \leq 0.05$. All data are presented as means ± standard error.

Results

Overexpression of SNAIL is sufficient to induce EndMT

SNAIL expression has been shown to be essential for TGF-β-induced EndMT in embryonic endothelial cells [2] and human cutaneous microvascular endothelial cells [19]. However, it is unknown whether such a requirement extends to EndMT of all endothelial cell types. We recently reported that individual endothelial cell types respond differently to TGF-β2 [21], and this lead us to investigate whether induction of EndMT through SNAIL overexpression applies equally to endothelial cells harvested

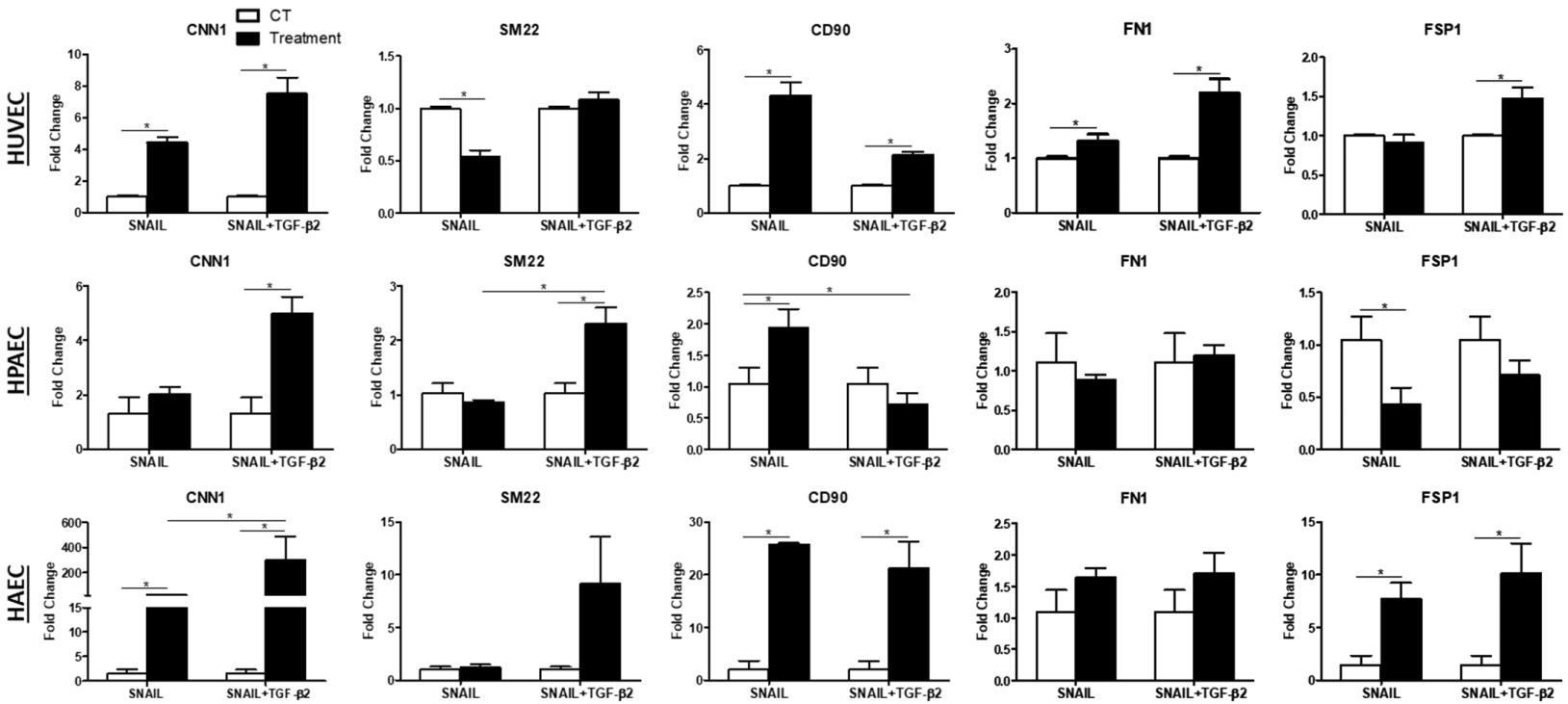

Figure 2. Effect of combined SNAIL overexpression and TGF-β2 treatment on the expression of mesenchymal markers in human endothelial cells from different anatomical origins. Expression analysis of mesenchymal markers CNN1, SM22, CD90, FN1 and FSP1 in HUVEC, HPAEC, and HAEC by qPCR after EndMT induction by SNAIL overexpression (SNAIL) and combined SNAIL overexpression and TGF-β2 treatment (SNAIL+TGF-β2). Results are expressed as log fold-changes relative to control (CT) after normalization to at least two endogenous control genes (n = 3-4, *P ≤ 0.05).

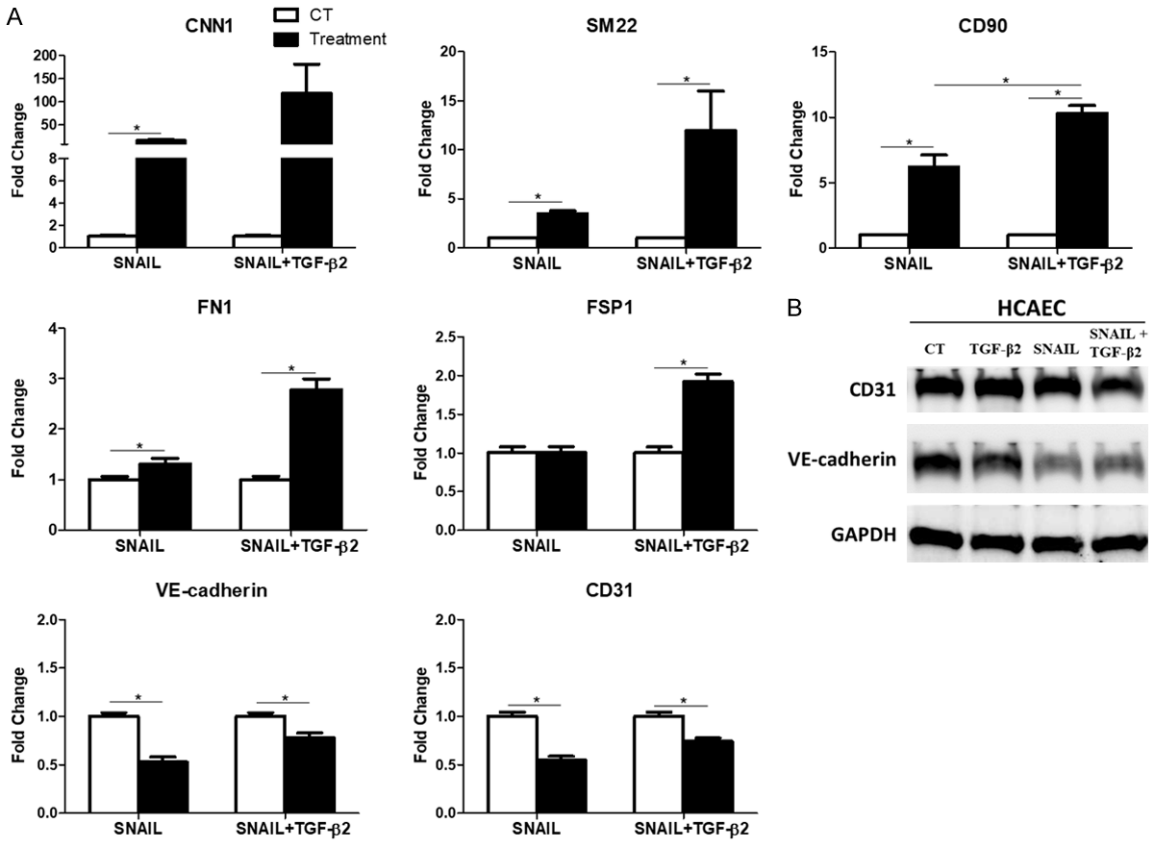

Figure 3. Expression of endothelial and mesenchymal markers in HCAEC after EndMT induction by combined SNAIL overexpression and TGF-β2 treatment. A. qPCR analysis of endothelial (CD31 and VE-cadherin) and mesenchymal (CNN1, SM22, CD90, FN1, and FSP1) genes in control (CT), SNAIL overexpression (SNAIL) and combined SNAIL+TGF-β2 treatment. Results are expressed as log fold-change relative to control (CT) after normalization to at least two endogenous control genes (n = 3-4, *P ≤ 0.05). B. Representative Western blot image comparing changes in the expression of CD31 and VE-cadherin. TGF-β2 treatment was used as positive control.

from different tissues. We overexpressed SNAIL in endothelial cells isolated from different vascular beds (umbilical vein, pulmonary, aortic, and coronary artery) and compared EndMT marker expression during transition. Our results show that individual endothelial cell cultures responded differently to SNAIL overexpression in a way that depended on the cell origin and marker under test (**Figure 1**). Human aortic (HAECs) and coronary artery (HCAECs) endothelial cells were the most responsive, showing significant changes in the expression of mesenchymal markers, CNN1 (20.51 ± 4.87-fold and 16.23 ± 2.00-fold, respectively, P ≤ 0.05) and CD90 (25.78 ± 0.28-fold and 6.02 ± 0.91-fold, respectively, P ≤ 0.05). HAECs also showed an increase in FSP1 (7.69 ± 1.55-fold, P ≤ 0.05) while HCAECs showed upregulation of SM22 (3.47 ± 0.29-fold, P ≤ 0.05) and FN1 (1.30 ± 0.11-fold, P ≤ 0.05). Moreover, SNAIL overexpression in HCAECs was sufficient to promote the expected decrease in endothelial cell markers CD31 (0.55 ± 0.04-fold, P ≤ 0.05) and VE-cadherin (0.53 ± 0.05-fold, P ≤ 0.05) during EndMT. Similar reductions of endothelial cell markers were observed in HAECs, although the results were not significant.

Interestingly, SM22 expression in HUVECs was significantly reduced (0.53 ± 0.06-fold, P ≤ 0.05) by overexpression of SNAIL while other markers were induced (CNN1: 4.40 ± 0.35-fold; CD90: 4.32 ± 0.48-fold; FN1: 1.31 ± 0.12-fold, P ≤ 0.05). In HPAECs, the effects of SNAIL overexpression were limited to induction of CD90 (1.93 ± 0.30-fold, P ≤ 0.05) and decrease in FSP1 (0.43 ± 1.56-fold, P ≤ 0.05). These results demonstrate differential responses to SNAIL overexpression that are associated with cell type and the individual EndMT marker expression.

Combination of SNAIL overexpression and TGF-β2 treatment potentiates EndMT

Because SNAIL overexpression differentially affects the induction of EndMT in endothelial cells from different anatomical origins, we investigated how a combination of SNAIL overexpression and TGF-β2 treatment may potentiated the transition.

Combination treatment had only modest effects on HUVECs, conferring increased expression of CNN1 (7.51 ± 1.02-fold, $P \leq 0.05$), CD90 (2.12 ± 0.12-fold, $P \leq 0.05$), FN1 (2.18 ± 0.26-fold, $P \leq 0.05$), and FSP1 (1.48 ± 0.14-fold, $P \leq 0.05$), that were not significantly different from single treatments (**Figure 2**). In HPAECs, the expression of mesenchymal markers CNN1 (4.98 ± 0.62-fold, $P \leq 0.05$) and SM22 (2.31 ± 0.29-fold, $P \leq 0.05$) was enhanced by combined treatment, but other markers remained unchanged compared with single treatments (**Figure 2**). Combined TGF-β2 and SNAIL overexpression in HAECs was sufficient to promote an increase in CNN1 (299.15 ± 187.62-fold, $P \leq 0.05$), CD90 (21.24 ± 5.07-fold, $P \leq 0.05$), and FSP1 (10.12 ± 2.86-fold, $P \leq 0.05$) but was without additional effects on other markers (**Figure 2**). There were no significant differences in the expression of endothelial markers in HUVECs, HPAECs, and HAECs (data not shown).

The impact of combination treatment on the induction of EndMT was most pronounced in HCAECs (**Figure 3A**). Compared to control and individual treatments, the combination conferred enhanced upregulation of the expression of all mesenchymal markers tested, including CNN1 (118.16 ± 62.95-fold, $P = 0.0681$), SM22 (11.96 ± 4.00-fold, $P \leq 0.05$), CD90 (10.32 ± 0.57-fold, $P \leq 0.05$), FN1 (2.78 ± 0.22-fold, $P \leq 0.05$), and FSP1 (1.92 ± 0.09-fold, $P \leq 0.05$). In addition to this, the combined treatment significantly reduced the expression of endothelial markers CD31 (0.74 ± 0.03-fold, $P \leq 0.05$) and VE-cadherin (0.78 ± 0.05-fold, $P \leq 0.05$) in a manner similar to SNAIL overexpression alone.

Enhanced induction of EndMT markers in HCAECs by combination treatment was confirmed by western blots (**Figure 3B**).

Taken together, our results suggest that SNAIL overexpression combined with TGF-β2 treatment is a stronger stimulus for EndMT in HCAECs compared with other endothelial cell types.

Global gene expression in HCAEC after EndMT induction

To better understand the differences between treatments on EndMT induction, we performed microarray analysis of HCAECs overexpressing SNAIL alone and in combination with TGF-β2 treatment. Results were compared to untreated and empty vector controls. Hierarchical clustering analysis of global gene expression patterns separated all groups into two major branches. Untreated samples clustered together with empty vector controls, while all SNAIL overexpression samples clustered together, including those with the combined treatment (**Figure 4A**).

We next determined the number of differentially expressed genes comparing all treatment groups (**Figure 4B**). There were no significant differences in gene expression between untreated and empty vector controls, with the exception of RDH16, that was subject to a 2.19-log fold increase. SNAIL overexpression triggered changes in the expression of 541 genes relative to the untreated control group (352 genes up-regulated and 189 genes down-regulated), while combined SNAIL overexpression plus TGF-β2 treatment increased this number to 659 genes (379 genes up-regulated and 280 genes down-regulated). Combined treatment promoted changes in the expression of only 20 genes relative to SNAIL overexpression alone (8 genes up-regulated and 12 genes down-regulated). These results suggest that SNAIL exerts global regulation of EndMT genes while the addition of TGF-β2 in combination treatment modulates and potentiates the effects of SNAIL while exerting independent effects on selective genes.

We assessed the top 100 differentially expressed genes altered by SNAIL overexpression relative to untreated control (**Table 1**) and found an increase in the expression of collagens including COL1A1 (3.74-log fold change, $P = 0.003$) and COL1A2 (2.95-log fold change, $P = 0.0005$) and a decrease of cell junction genes, such as keratin (KRT19, -2.96-log fold change, $P = 4.24e\text{-}08$) and claudin (CLDN5, -2.00-log fold change, $P = 1.02e\text{-}06$).

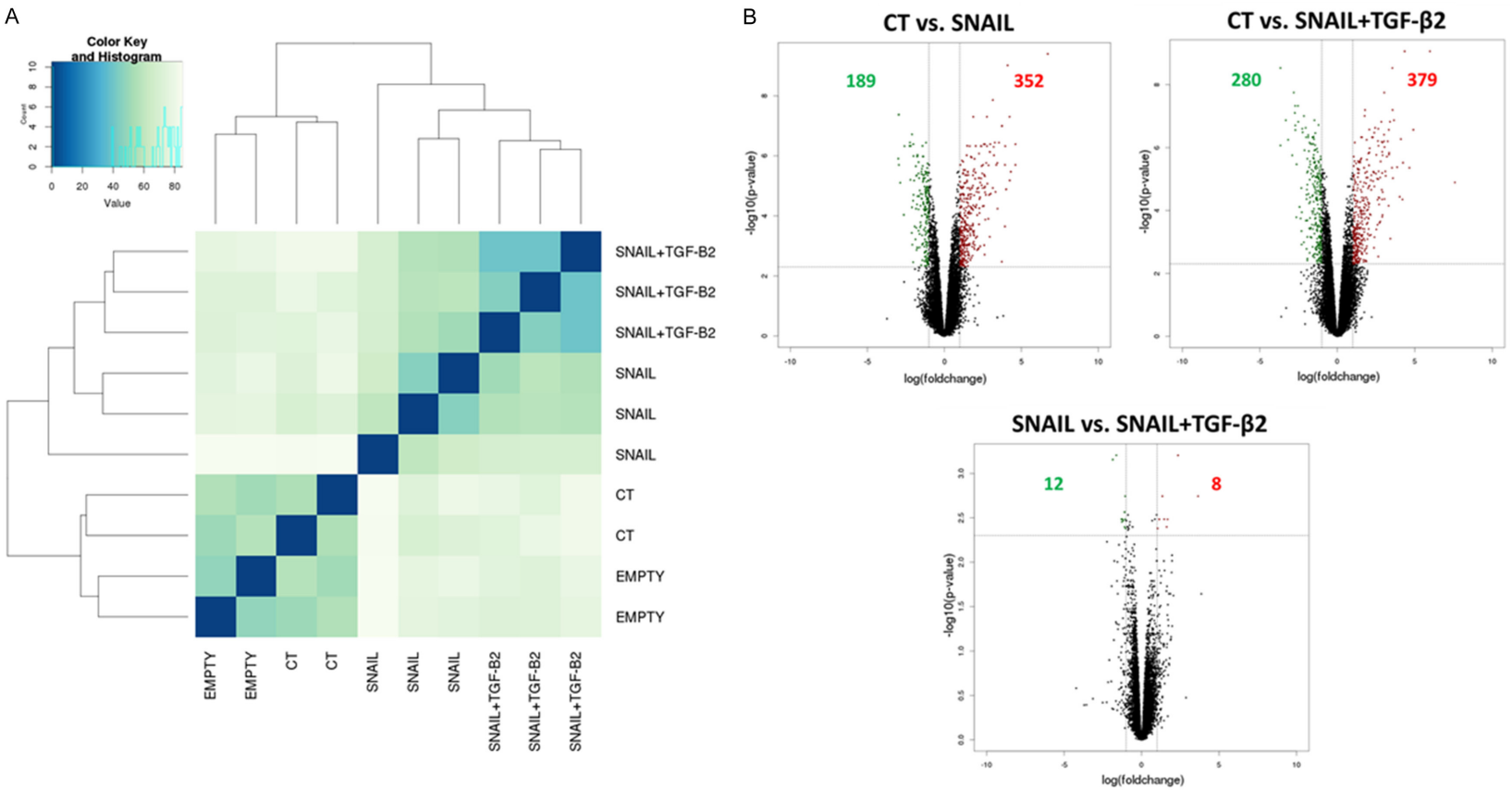

Figure 4. Gene expression profiling of HCAEC after induction of EndMT. A. Correlation matrix showing similarities in transcription profiles among experimental groups. B. Volcano Plot showing differential gene expression between sample groups. A total of 541 genes were differently expressed between CT and SNAIL groups; 659 between CT and SNAIL+TGF-β2 groups and 20 between SNAIL and SNAIL+TGF-β2 groups. Upregulated genes are shown on the upper right side (red), while downregulated genes are shown on the upper left side (green). Dots in the middle of the figure represent genes for which the expression showed no statistical difference. CT, untreated control (n = 2); Empty, empty vector control (n = 2); SNAIL, SNAIL overexpression (n = 3); SNAIL+TGF-β2, SNAIL overexpression plus TGF-β2 treatment (n = 3).

Table 1. Top genes differentially expressed between HCAEC untreated control and SNAIL overexpression in microarray analysis

50 genes up regulated in SNAIL				50 genes down regulated in SNAIL			
Genes	Log fold change	Genes	Log fold change	Genes	Log fold change	Genes	Log fold change
RDH16	6.72	SNAR-A3	2.96	ADAMTS18	-2.99	FLJ41200	-1.82
C3orf83	4.62	COL1A2	2.95	KRT19	-2.96	LCN6	-1.81
SPINT2	4.62	IFIT3	2.91	LYPD1	-2.95	CGNL1	-1.80
MX1	4.32	SNAR-B2	2.87	ADIRF	-2.86	DNER	-1.78
IFIT1	4.25	OASL	2.86	LOX	-2.63	CHN1	-1.77
XLOC_007191	4.23	SCG5	2.79	PDGFRL	-2.59	FUT1	-1.77
S100A2	4.11	SERPINF1	2.77	ATP6V0A4	-2.27	NSG1	-1.75
IFI44L	4.02	REEP2	2.76	KRT19P2	-2.24	LAMP3	-1.74
MMP24	3.96	NUPR1	2.72	NOV	-2.20	A33P3240078	-1.74
GAL	3.94	BEX1	2.70	NQO1	-2.18	BIRC3	-1.74
CD69	3.93	CMPK2	2.66	NTN4	-2.12	IGFBP2	-1.68
LCN15	3.74	SPON2	2.64	SYBU	-2.10	FRAS1	-1.68
COL1A1	3.74	ENST00000433933	2.63	TMEM106C	-2.10	ECHDC2	-1.67
BSPRY	3.54	CHRNB1	2.63	MEDAG	-2.08	CCL14	-1.67
RFPL4AL1	3.45	ISG15	2.63	GNAZ	-2.03	ACP5	-1.64
IFI6	3.44	CNN1	2.62	COL13A1	-2.03	PRSS3	-1.64
SNAR-G2	3.37	EDN2	2.61	CRTAC1	-2.02	SLC7A11	-1.61
IFITM1	3.32	UBD	2.59	HS3ST1	-2.01	DDIT4L	-1.61
SNAR-F	3.28	OAS1	2.59	CLDN5	-2.00	PRSS2	-1.60
SNAR-D	3.22	BAIAP2L1	2.57	BEX5	-1.97	FAM110D	-1.58
SNAR-H	3.21	UCP2	2.56	TNFSF15	-1.93	RNASE4	-1.55
RNF112	3.15	CD200	2.51	METTL7A	-1.88	LINC00520	-1.55
PLEKHA4	3.14	BATF2	2.50	ENO2	-1.86	IL3RA	-1.55
EPN3	3.01	FABP4	2.48	UNC5B-AS1	-1.84	ELFN2	-1.53
HSD11B1	2.98	FAM71E1	2.46	CASP5	-1.82	EDIL3	-1.51

We also assessed the top 100 differentially expressed genes altered by the combination SNAIL-TGF-β2 treatment relative to untreated control (**Table 2**). We found that gene expression profiles in the combined treatment were similar to SNAIL alone, including increased expression of collagens markers (COL1A1, 7.59-log fold change, P = 1.27e-05; COL1A2, 4.02-log fold change, P = 3.67e-05) and decrease of cell junctions genes (KRT19, -3.67-log fold change, P = 2.93e-09; CLDN5, -2.23-log fold change, P = 3.27e-07) in combined treatment. COL1A1 and COL1A2 gene expression was further validated by qPCR and western blot (**Figure 5A**, **5B**, **5G**). In addition, we observed an increase in other EndMT markers and inducers by the combined treatment, including calponin (CNN1, 4.21-log fold change, P = 4.45e-05), SM22 (TAGLN, 2.93-log fold change, P = 2.61e-05), TGFB1 (2.92-log fold change, P = 1.75e-06), and TGFB2 (2.66-log fold change, P = 3.86e-05) (**Table 2**). Our results suggest that SNAIL alone is a potent inducer of EndMT, however, when SNAIL is combined with TGF-β2 EndMT is potentiated at least in part by upregulation of TGF-β family members.

Pathway prediction analysis reveals that different target genes are activated by combined SNAIL overexpression plus TGF-β2 treatment relative to single treatment

Because combined SNAIL overexpression and TGF-β2 treatment showed the strongest effect on EndMT in HCAECs, we performed pathway analysis to identify potential signaling mechanisms that are differentially expressed in combined versus single treatment. Using Ingenuity Pathway Analysis software, we were able to identify several pathways based on our micro-

Table 2. Top genes differentially expressed between HCAEC untreated control and combined SNAIL overexpression plus TGF-β2 treatment (SNAIL+TGF-β2) in microarray analysis

50 genes up regulated in SNAIL+TGF-β2				50 genes down regulated in SNAIL+TGF-β2			
Genes	Log fold change	Genes	Log fold change	Genes	Log fold change	Genes	Log fold change
COL1A1	7.59	SNAR-B2	3.05	ADIRF	-3.67	TCN2	-2.04
RDH16	5.98	MX1	3.04	KRT19	-3.67	G0S2	-2.02
GAL	4.91	REEP2	3.03	CXCL1	-3.32	IGFBP1	-2.02
AMTN	4.65	SNAR-F	3.02	ADAMTS18	-3.18	COL13A1	-1.99
S100A2	4.35	SNAR-H	3.01	LYPD1	-2.90	LINC01088	-1.98
SPINT2	4.24	TAGLN	2.93	LAMP3	-2.80	CDH4	-1.98
CNN1	4.21	TGFBI	2.92	IGFBP2	-2.74	ELFN2	-1.97
C3orf83	4.11	LOC729444	2.92	KRT19P2	-2.72	BEX5	-1.95
COL1A2	4.02	NUPR1	2.91	IL1RL1	-2.72	LCN6	-1.94
FOXS1	3.86	SPON2	2.91	PDGFRL	-2.71	LINC00176	-1.93
XLOC_007191	3.66	CLDN4	2.91	IL8	-2.65	GNAZ	-1.93
GREM1	3.59	IFI44L	2.90	CXCL2	-2.62	CGNL1	-1.93
SERPINF1	3.57	XLOC_004049	2.89	CRTAC1	-2.55	ACKR3	-1.93
RNF112	3.56	EPN3	2.87	ATP6V0A4	-2.51	NOV	-1.93
GDF6	3.54	SNAR-A3	2.86	BIRC3	-2.44	ACP5	-1.91
SAA1	3.43	CRIP1	2.84	LOX	-2.37	FRAS1	-1.88
LCN15	3.40	LBH	2.80	SYBU	-2.32	NSG1	-1.88
IL11	3.34	POSTN	2.77	CSF3	-2.31	IL3RA	-1.86
SNAR-G2	3.34	CST6	2.77	XLOC_006681	-2.30	DPP4	-1.83
BSPRY	3.33	OXTR	2.72	METTL7A	-2.29	FLJ41200	-1.81
RFPL4AL1	3.31	ITGA11	2.72	NQO1	-2.25	UNC5B-AS1	-1.80
SNAR-D	3.25	RRAD	2.69	CLDN5	-2.23	FZD9	-1.80
MMP24	3.20	TGFB2	2.66	CXCL6	-2.16	CLU	-1.79
BAIAP2L1	3.13	FABP4	2.66	TMEM106C	-2.15	SLC37A1	-1.79
BEX1	3.10	CD200	2.66	PSG8	-2.11	SERPIND1	-1.78

array data that were common to single and combined treatment groups and also specific for individual groups. Selected pathways we found to be relevant are shown in **Table 3**. Several biological processes were common to both treatment groups when compared to control. The top ranked pathways activated in both treatment groups include genes associated with cancer, extracellular-matrix composition (COL1A1, COL1A2, and COL13A), inflammation (CXCL12, SELE) and regulation of epithelial-mesenchymal transition (EMT) (FZD2, HMGA2, LOX, NOTCH3, NOTCH4, and TGFB2). Interestingly, in some cases, the identity of the genes showing altered expression in biological processes common to both groups, were dependent of the treatment. In the biological process "Regulation of EMT", SNAIL overexpression alone affected the expression of FGF2 (1.12-log fold change, P = 0.0007), FGFR3 (1.09-log fold change, P = 0.0003), and FZD8 (-1.14-log fold change, P = 2.87e-05), targets that were not altered by the combination treatment. Similarly, the combination treatment in this same category, induced additional changes in the expression of FZD9 (-1.80-log fold change, P = 0.0003), MMP2 (1.19-log fold change, P = 1.30e-05), SMAD3 (-1.06-log fold change, P = 2.34e-06), and WNT5B (1.88-log fold change, P = 0.001), which were not changed in the single treatment group. The biological processes specifically associated with SNAIL overexpression alone were related to growth (CDC42 signaling), DNA damage (GADD45 signaling), cell junction (Tight junction signaling), and chemokine (IL-10 signaling), while those associated with combined SNAIL overexpression and TGF-β2 treatment were related to extracellular-matrix remodeling (inhibition of metalloproteases) and inflammation (IL-8, IL-12, IGF-1, and TREM-1

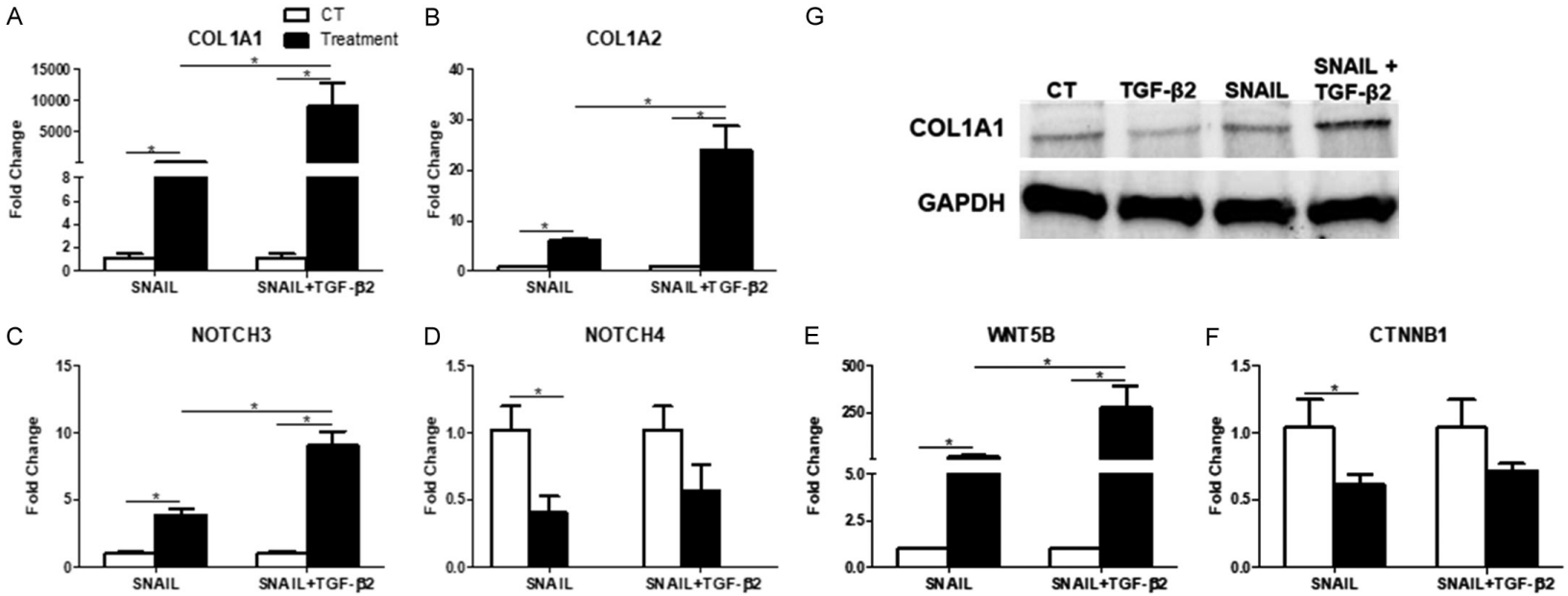

Figure 5. Validation of selected differently expressed genes identified by microarray analysis of HCAEC after EndMT induction. A-F. qPCR analysis of NOTCH3, NOTCH4, WNT5B, CTNNB1, COL1A1 and COL1A2. Results are expressed as log fold-changes relative to control after normalization to at least two endogenous control genes (n = 3-4, *P ≤ 0.05). G. Representative Western blot image showing changes in COL1A1 protein expression. GAPDH was used as loading control. TGF-β2 was used as positive control. CT, untreated control.

Table 3. Selected pathways expressed in HCAECs SNAIL overexpression and combined SNAIL overexpression plus TGF-β2 treatment (SNAIL+TGF-β2) in microarray analysis

Function	SNAIL		SNAIL+TGF-β2	
	Gene name	Fold change	Gene name	Fold change
Atherosclerosis signaling	APOD	2.13	APOD	1.56
	APOE	2.39	APOE	2.33
	CLU	-1.22	APOL1	-1.08
	COL1A1	3.74	CLU	-1.79
	COL1A2	2.95	COL1A1	7.58
	COL13A	-2.03	COL1A2	4.02
	CXCL12	2.28	COL13A	-1.98
	ITGA4	1.37	CXCL12	2.03
	LPL	1.31	ITGA4	2.52
	PLA2G16	-1.09	ITGB2	1.37
			LPL	1.32
			PLA2G16	-1.08
			RARRES3	-1.10
			RBP4	1.11
			SELE	-1.57
Regulation of EMT	FGF2	1.12	FZD2	1.76
	FGFR3	1.09	FZD9	-1.80
	FZD2	1.48	HMGA2	-1.15
	FZD8	-1.14	LOX	-2.36
	HMGA2	-1.12	MMP2	1.19
	LOX	-2.63	NOTCH3	1.89
	NOTCH3	1.63	NOTCH4	-1.01
	NOTCH4	-1.15	SMAD3	-1.06
	TGFB2	2.24	TGFB2	2.66
			WNT5B	1.88
Notch signaling	DLL4	-1.12	DLL4	-1.14
	NOTCH3	1.63	NOTCH3	1.89
	NOTCH4	-1.15	NOTCH4	-1.01
Molecular mechanisms of cancer	ARHGEF16	2.4	ARHGEF16	1.91
	BIRC3	-1.74	BIRC3	-2.44
	CCND2	2.32	BMP6	-1.02
	FZD2	1.48	CCND2	2.39
	GNAZ	-2.03	FZD2	1.76
	ITGA4	1.37	FZD9	-1.80
	MAPK13	1.32	GNAZ	-1.93
	PRKAR2B	-1.26	IRS1	1.01
	TGFB2	2.24	ITGA4	2.52
			LRP5	-1.14
			MAPK13	1.14
			PLCB4	1.95
			PRKAR2B	-1.48
			PRKCE	-1.03
			RAC2	-1.18
			SMAD3	-1.06
			TGFB2	2.66
			WNT5B	1.88

signaling). Considering the substantial effect of combined treatment on the EndMT induction in HCAECs relative to SNAIL alone, we identified 20 differently expressed genes specifically altered in the combined treatment group, (see **Table 4**). In the combined treatment we detected significantly increased expression of Fibulin-5 (FBLN5, 2.36-log fold change, P = 0.0006) and Fibroblast Activation Protein alpha (FAP, 1.13-log fold change, P = 0.003), which are known to initiate the EMT process. Our results suggest that SNAIL overexpression combined with TGF-β2 treatment induces the expression of genes essential for EndMT regulation.

Induction of EndMT by combined SNAIL overexpression and TGF-β2 treatment activates Notch and Wnt signaling pathways

Our microarrays revealed that members of the Notch and Wnt signaling pathway were differentially altered by SNAIL overexpression alone and in combination with TGF-β2. The Notch signaling pathway members DLL4, NOTCH3, and NOTCH4 were similarly induced in both treatment groups. The only member of the Wnt signaling pathway similarly altered in both groups was FZD2. FZD8 was specifically altered in the SNAIL overexpression group only, while FZD9 and WNT5B were altered only in the combined treatment group (**Table 3**). These differences may explain the

Tight junction signaling	CGN	1.79	CGN	1.91
	CLDN4	1.23	CLDN4	2.90
	CLDN5	-1.99	CLDN5	-2.23
	CLDN14	-1.30	PRKAR2B	-1.48
	MYLK	-1.01	TGFB2	2.66
	PRKAR2B	-1.26		
	TGFB2	2.24		

Table 4. Genes differentially expressed between HCAEC SNAIL overexpression and combined SNAIL overexpression plus TGF-β2 treatment (SNAIL+TGF-β2) in microarray analysis

Genes up regulated in SNAIL+TGF-β2		Genes down regulated in SNAIL+TGF-β2	
Genes	Log fold change	Genes	Log fold change
AMTN	3.65	CXCL1	-1.86
FBLN5	2.36	CBLN2	-1.63
CLDN4	1.68	IFI35	-1.30
TGFBI	1.62	DUSP5	-1.27
AMIGO2	1.46	IL1RL1	-1.24
SERPINE2	1.35	UBE2L6	-1.19
FAP	1.13	IGFBP1	-1.11
CLN8	1.03	OAS3	-1.10
		TRIB1	-1.09
		IGFBP2	-1.06
		LAMP3	-1.06
		LGALS9	-1.03

potentiation of EndMT induction promoted by combined treatment in HCAECs.

Therefore, we validated our findings by confirming the expression of some of these genes by qPCR in each group (**Figure 5**). NOTCH3 was upregulated by SNAIL overexpression alone (3.91 ± 0.41-fold, $P \leq 0.05$) and further increased by combined SNAIL plus TGF-β2 treatment (9.07 ± 1.01-fold, $P \leq 0.05$) (**Figure 5C**). NOTCH4 was downregulated by SNAIL alone (0.45 ± 0.16-fold, $P \leq 0.05$) and by combined SNAIL plus TGF-β2 treatment (0.57 ± 0.19-fold, $P = 0.07$), although this result was not significant (**Figure 5D**). WNT5B was significantly induced by SNAIL overexpression alone (19.05 ± 3.51-fold, $P \leq 0.05$) and further induced in the TGF-β2 combination treatment group (279.9 ± 112.7-fold, $P \leq 0.05$) (**Figure 5E**). Because Wnt5a can inhibit the Wnt/β-catenin pathway, we also analyzed the expression of CTNNB1 by qPCR and found that it was downregulated in all groups tested, but only significant in the single SNAIL overexpression treatment (0.54 ± 0.05-fold, $P \leq 0.05$) (**Figure 5F**). These results suggest that Notch and Wnt signaling pathways are involved in EndMT induction in HCAECs by SNAIL overexpression with or without TGF-β2.

Combined SNAIL overexpression plus TGF-β2 treatment increases cell migration

An important feature of cells undergoing mesenchymal transition is the acquisition of migration potential. We analyzed the effect of SNAIL overexpression alone or in combination with TGF-β2 on HCAECs potential to migrate using an *in vitro* scratch assay. Our results show that combined SNAIL overexpression and TGF-β2 treatment significantly increased cell migration by 24.40 ± 1.70%, $P \leq 0.05$ (**Figure 6**).

In order to define individual roles of SNAIL overexpression and combination treatments on migration, we analyzed related genes from microarrays. We observed several differentially expressed genes associated with extracellular-matrix remodeling, migration and invasion, including ADAM21 (1.63-log fold change, P = 0.0002), MMP2 (1.19-log fold change, P = 1.30e-05), MMP24 (3.20-log fold change, P = 1.94e-06), and EPCAM (1.74-log fold change, P = 0.0004). These analyses support roles for combined SNAIL overexpression and TGF-β2 treatment in EndMT and acquisition of the invasive phenotype.

Discussion

The results of our study show that endothelial cells from distinct anatomical locations respond differently to EndMT induction. We found that combined SNAIL overexpression and TGF-β2 treatment potently induced EndMT in HCAECs compared with SNAIL overexpression alone, and promoted a true phenotype characterized by decreased endothelial markers, increased mesenchymal markers and enhanced cell migration. We have also showed that Notch and non-canonical Wnt signaling pathways are upregulated in parallel.

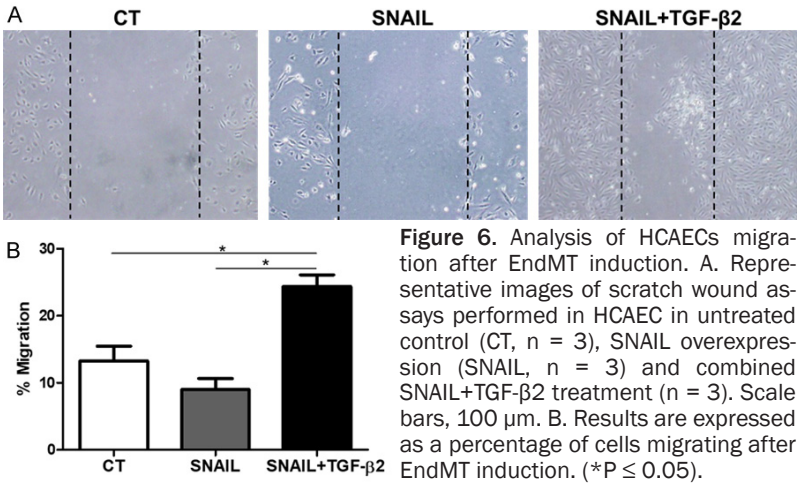

Figure 6. Analysis of HCAECs migration after EndMT induction. A. Representative images of scratch wound assays performed in HCAEC in untreated control (CT, n = 3), SNAIL overexpression (SNAIL, n = 3) and combined SNAIL+TGF-β2 treatment (n = 3). Scale bars, 100 μm. B. Results are expressed as a percentage of cells migrating after EndMT induction. (*P ≤ 0.05).

It is well-known that the vascular system is diverse in structure, architecture, and physiology [20]. Studies have shown that ECs from large- and micro-vessels isolated from different tissues have distinctive characteristics and gene expression profiles [20]. In our study, we observed that SNAIL overexpression was sufficient to induce EndMT in HCAECs, and this effect was significantly enhanced when combined with TGF-β2 treatment. Medici and colleagues recently reported that human cutaneous microvascular endothelial cells treated with TGF-β2 undergo SNAIL-mediated EndMT [19]. However, in contrast to our results they found that SNAIL overexpression alone was insufficient to induce EndMT and, there was no change in the expression of endothelial and mesenchymal markers [19]. The apparent discrepancy may be due to the fact that Medici and colleagues used cutaneous microvascular endothelial cells while in our study we used HCAECs.

To elucidate potential mechanisms governing the differential effects of treatments on EndMT induction in HCAECs we performed gene expression profiling by microarray. Hierarchical clustering showed that SNAIL overexpression samples clustered away from controls, suggesting that SNAIL triggers gene expression changes. We identified 20 differentially expressed genes when SNAIL alone was compared with the combined treatment. Among these genes, we identified significantly increased expression of *FBLN5* and *FAP* in the combined treatment group. *FBLN5* is a member of the Fibulin family of extracellular-matrix proteins that was first identified by its role in the phenotypic modulation of vascular smooth muscle cells (SMCs) [23, 24]. FBLN5 has been shown to mediate cell-cell and cell-matrix signaling coupled to the regulation of tissue development, remodeling and repair [25]. Moreover, it has been reported that FBLN5 initiates and enhances TGF-β-mediated EMT in normal and malignant mammary epithelial cells, suggesting that FBLN5 may be an important regulator of normal EMT during embryonic development, as well as an inducer of oncogenic EMT during the development and progression of human breast cancers [25]. *FAP* expression is known to be upregulated during tissue repair [26], pathological fibrosis [27, 28] and in tumors [29], and thought to control fibroblast growth or epithelial-mesenchymal interactions [30]. Therefore, the increase of *FBLN5* and *FAP* expression in our combined treatment group suggests that induction of EndMT may be a central mechanism for cancer progression.

Pathway analyses to detect potential signaling mechanisms that are involved in SNAIL-mediated induction of EndMT showed that SNAIL alone or in combination with TGF-β2 triggers similar functional activation traits, that are related to epithelial-mesenchymal transition, tight junctions, cancer, and Notch signaling. However, within these pathways, the gene expression signatures were different and dependent on the specific treatment. The combined treatment caused gene expression changes related to several pro-inflammatory pathways mediated by IGF-1, IL-8, IL-12 and TREM-1, which were not found in single treatment samples. These results could explain the potentiation of EndMT induction by the combined treatment.

Insulin-like growth factor-I (IGF-I) has been shown to inhibit EndMT [31], while the IGF-IR/ligand system can initiate EMT progression and increase the metastatic potential of prostate, breast, and gastric cancer cells [32-35]. A role for IL-8 has also been described in EMT and EndMT. IL-8 induces EMT of Renal cell carcinoma (RCC) through the activation of the AKT

signaling pathway, providing a potential molecular mechanism for RCC metastasis [36]. In EndMT, the expression of IL-8 was greatly increased during safrole oxide-induced EndMT [37]. In addition, Good and colleagues quantified the secretion of inflammatory cytokines from EndMT cells. They showed that EndMT cells secreted significantly higher levels of inflammatory cytokines including IL-4, IL-13, IL-6, IL-8, and TNFα [38]. Although previous work described roles for IGF-1 and IL-8 in EMT and EndMT, our present study is the first to relate IL-12 and TREM-1 to EndMT.

Our results also shown that combined SNAIL overexpression and TGF-β2 treatment significantly increased cell migration and the expression of related genes. In our microarray data, we observed increase expression of ADAM21, MMP2, MMP24, and EPCAM. The MMP family has previously been shown to induce EMT in variety of cancers. Jia and colleagues reported that three MMP family members (MMP2, MMP7, and MMP14) were decreased in KIAA1199 knockdown gastric cancer cells, suggesting that KIAA1199 induces migration and invasion by increase MMPs expression, which could also promote EMT progression [39]. Moreover, another study showed that EPCAM short interfering RNAs significantly decreased the invasion and migration potentials of breast cancer cell lines [40]. Thus, the increase of ADAM21, MMP2, MMP24, and EPCAM expression in the combined treatment is consistent with the migratory capacity of these cells.

Notch and Wnt signaling pathways have been implicated in EndMT induction [41-43]. Noseda and colleagues have shown that overexpression of Notch1 and Notch4 conferred EndMT in different types of endothelial cells [41]. Moreover, Wnt3a has also been shown to induce EndMT in human dermal microvascular endothelial cells through upregulation of SLUG [42]. We found that WNT5B is significantly induced by combined SNAIL and TGF-β2 treatment in HCAECs, but remained unchanged in single treatment samples. The involvement of WNT5B in EndMT is supported by recent work showing that exogenous treatment of lymphatic endothelial cells with recombinant WNT5B triggers EndMT, associated with upregulation of SNAIL and SLUG [43]. The level of induction in WNT5B expression by combined SNAIL overexpression and TGF-β2 signaling was remarkably high relative to all other members of both Notch and Wnt pathways together, suggesting an important role for this molecule in the induction of EndMT in HCAECs. In fact, increased WNT5B expression positively correlates with valve calcification, fibrosis, inflammation, lipids, and neovascularization. One study revealed that WNT5B is highly expressed in severely calcified valves, with immunoreactivity in valvular interstitial cells (VICs) on both the aortic and ventricular sides of the valve leaflet [44].

Identification of potential mechanisms controlling phenotypic changes mediated by EndMT may lead to novel therapeutic approaches for diseases such as cancer and tissue fibrosis. In the present work, we demonstrated for the first time that combined SNAIL overexpression and TGF-β2 treatment is a potential tool to investigate EndMT in HCAECs. Importantly, we show that the mechanisms involved in EndMT are tissue specific and depend on the cell type involved. Therefore, one protocol does not fit all endothelial cell types, suggesting the relevance and need for standardized methods to perform studies in this field.

Acknowledgements

We would like to thank Dr. Keith A. Webster for critical reading and editing of this manuscript. We thank Ms. Patrícia V. B. Palma for assistance with flow cytometry and Ms. Amelia G. de Araujo for assistance with the microarray technique. We thank Dr. Robert A. Weinberg and Dr. Leonardo Rodrigues, Whitehead Institute for Biomedical Research, Cambridge, MA, for kindly providing us with the plasmid DNA used for generation of SNAIL lentivirus. This work was supported by Center for Cell-based Therapy-CTC CEPID (FAPESP/n°2013/08135-2), Fundação Hemocentro de Ribeirão Preto (FUNDHERP), Centro Regional de Hemoterapia de Ribeirão Preto (CRH), Fundação de Amparo à Pesquisa do Estado de São Paulo (FAPESP), Coordenação de Aperfeiçoamento de Pessoal de Nível Superior (CAPES), and Conselho Nacional de Desenvolvimento Científico e Tecnológico (CNPq). Pinto, M.T. was a fellow of the FAPESP (FAPESP/n°2011/21740-7).

Disclosure of conflict of interest

None.

Address correspondence to: Simone Kashima, National Institute of Science and Technology in Stem Cell and Cell Therapy, Center for Cell-Based Therapy and Regional Blood Center of Ribeirão Preto, Tenente Catão Roxo Street, 2501, 14051-140

- Ribeirão Preto, São Paulo, Brazil. Tel: +55(16)2101-9300 Ext. 9311; Fax: +55(16)2101-9309; E-mail: skashima@hemocentro.fmrp.usp.br

References

[1] He J, Xu Y, Koya D, Kanasaki K. Role of the endothelial-to-mesenchymal transition in renal fibrosis of chronic kidney disease. Clin Exp Nephrol 2013; 17: 488-497.

[2] Kokudo T, Suzuki Y, Yoshimatsu Y, Yamazaki T, Watabe T, Miyazono K. Snail is required for TGFbeta-induced endothelial-mesenchymal transition of embryonic stem cell-derived endothelial cells. J Cell Sci 2008; 121: 3317-3324.

[3] Medici D, Kalluri R. Endothelial-mesenchymal transition and its contribution to the emergence of stem cell phenotype. Semin Cancer Biol 2012; 22: 379-384.

[4] Piera-Velazquez S, Li Z, Jimenez SA. Role of endothelial-mesenchymal transition (EndoMT) in the pathogenesis of fibrotic disorders. Am J Pathol 2011; 179: 1074-1080.

[5] Potenta S, Zeisberg E, Kalluri R. The role of endothelial-to-mesenchymal transition in cancer progression. Br J Cancer 2008; 99: 1375-1379.

[6] Eisenberg LM, Markwald RR. Molecular regulation of atrioventricular valvuloseptal morphogenesis. Circ Res 1995; 77: 1-6.

[7] Zeisberg EM, Potenta S, Xie L, Zeisberg M, Kalluri R. Discovery of endothelial to mesenchymal transition as a source for carcinoma-associated fibroblasts. Cancer Res 2007; 67: 10123-10128.

[8] Zeisberg EM, Tarnavski O, Zeisberg M, Dorfman AL, McMullen JR, Gustafsson E, Chandraker A, Yuan X, Pu WT, Roberts AB, Neilson EG, Sayegh MH, Izumo S, Kalluri R. Endothelial-to-mesenchymal transition contributes to cardiac fibrosis. Nat Med 2007; 13: 952-961.

[9] Zeisberg EM, Potenta SE, Sugimoto H, Zeisberg M, Kalluri R. Fibroblasts in kidney fibrosis emerge via endothelial-to-mesenchymal transition. J Am Soc Nephrol 2008; 19: 2282-2287.

[10] Hashimoto N, Phan SH, Imaizumi K, Matsuo M, Nakashima H, Kawabe T, Shimokata K, Hasegawa Y. Endothelial-mesenchymal transition in bleomycin-induced pulmonary fibrosis. Am J Respir Cell Mol Biol 2010; 43: 161-172.

[11] Lee JG, Kay EP. FGF-2-induced wound healing in corneal endothelial cells requires Cdc42 activation and Rho inactivation through the phosphatidylinositol 3-kinase pathway. Invest Ophthalmol Vis Sci 2006; 47: 1376-86.

[12] Armstrong EJ, Bischoff J. Heart valve development: endothelial cell signaling and differentiation. Circ Res 2004; 95: 459-470.

[13] Azhar M, Runyan RB, Gard C, Sanford LP, Miller ML, Andringa A, Pawlowski S, Rajan S, Doetschman T. Ligand-specific function of transforming growth factor beta in epithelial-mesenchymal transition in heart development. Dev Dyn 2009; 238: 431-442.

[14] Medici D, Hay ED, Olsen BR. Snail and slug promote epithelial-mesenchymal transition through beta-catenin-T-cell factor-4-dependent expression of transforming growth factor-beta3. Mol Biol Cell 2008; 19: 4875-87.

[15] Liebner S, Cattelino A, Gallini R, Rudini N, Iurlaro M, Piccolo S, Dejana E. β-catenin is required for endothelial-mesenchymal transformation during heart cushion development in the mouse. J Cell Biol 2004; 166: 359-367.

[16] Parker BS, Argani P, Cook BP, Liangfeng H, Chartrand SD, Zhang M, Saha S, Bardelli A, Jiang Y, St Martin TB, Nacht M, Teicher BA, Klinger KW, Sukumar S, Madden SL. Alterations in vascular gene expression in invasive breast carcinoma. Cancer Res 2004; 64: 7857-66.

[17] Zidar N, Gale N, Kojc N, Volavsek M, Cardesa A, Alos L, Höfler H, Blechschmidt K, Becker KF. Cadherin-catenin complex and transcription factor Snail-1 in spindle cell carcinoma of the head and neck. Virchows Arch 2008; 453: 267-74.

[18] Schwock J, Bradley G, Ho JC, Perez-Ordonez B, Hedley DW, Irish JC, Geddie WR. SNAI1 expression and the mesenchymal phenotype: an immunohistochemical study performed on 46 cases of oral squamous cell carcinoma. BMC Clin Pathol 2010; 10: 1.

[19] Medici D, Potenta S, Kalluri R. Transforming growth factor-β2 promotes Snail-mediated endothelial-mesenchymal transition through convergence of Smad-dependent and smad-independent signalling. Biochem J 2011; 437: 515-520.

[20] Chi JT, Chang HY, Haraldsen G, Jahnsen FL, Troyanskaya OG, Chang DS, Wang Z, Rockson SG, van de Rijn M, Botstein D, Brown PO. Endothelial cell diversity revealed by global expression profiling. Proc Natl Acad Sci U S A 2003; 100: 10623-10628.

[21] Pinto MT, Covas DT, Kashima S, Rodrigues CO. Endothelial mesenchymal transition: comparative analysis of different induction methods. Biol Proced Online 2016; 18: 10.

[22] Pfaffl MW. A new mathematical model for relative quantification in real-time RT-PCR. Nucleic Acids Res 2001; 29: e45.

[23] Kowal RC, Richardson JA, Miano JM, Olson EN. EVEC, a novel epidermal growth factor-like repeat-containing protein upregulated in embryonic and diseased adult vasculature. Circ Res 1999; 84: 1166-76.

[24] Nakamura T, Ruiz-Lozano P, Lindner V, Yabe D, Taniwaki M, Furukawa Y, Kobuke K, Tashiro K,

Lu Z, Andon NL, Schaub R, Matsumori A, Sasayama S, Chien KR, Honjo T. DANCE, a novel secreted RGD protein expressed in developing, atherosclerotic, and balloon-injured arteries. J Biol Chem 1999; 274: 22476-83.

[25] Lee YH, Albig AR, Regner M, Schiemann BJ, Schiemann WP. Fibulin-5 initiates epithelial-mesenchymal transition (EMT) and enhances EMT induced by TGF-beta in mammary epithelial cells via a MMP-dependent mechanism. Carcinogenesis 2008; 29: 2243-51.

[26] Ghersi G, Dong H, Goldstein LA, Yeh Y, Hakkinen L, Larjava HS, Chen WT. Regulation of fibroblast migration on collagenous matrix by a cell surface peptidase complex. J Biol Chem 2002; 277: 29231-41.

[27] Levy MT, McCaughan GW, Marinos G, Gorrell MD. Intrahepatic expression of the hepatic stellate cell marker fibroblast activation protein correlates with the degree of fibrosis in hepatitis C virus infection. Liver 2002; 22: 93-101.

[28] Wang XM, Yao TW, Nadvi NA, Osborne B, McCaughan GW, Gorrell MD. Fibroblast activation protein and chronic liver disease. Front Biosci 2008; 13: 3168-80.

[29] Henriksson ML, Edin S, Dahlin AM, Oldenborg PA, Öberg Å, Van Guelpen B, Rutegård J, Stenling R, Palmqvist R. Colorectal cancer cells activate adjacent fibroblasts resulting in FGF1/FGFR3 signaling and increased invasion. Am J Pathol 2011; 178: 1387-94.

[30] Scanlan MJ, Raj BK, Calvo B, Garin-Chesa P, Sanz-Moncasi MP, Healey JH, Old LJ, Rettig WJ. Molecular cloning of fibroblast activation protein alpha, a member of the serine protease family selectively expressed in stromal fibroblasts of epithelial cancers. Proc Natl Acad Sci U S A 1994; 91: 5657-61.

[31] Zhang Z, Zhang T, Zhou Y, Wei X, Zhu J, Zhang J, Wang C. Activated phosphatidylinositol 3-kinase/Akt inhibits the transition of endothelial progenitor cells to mesenchymal cells by regulating the forkhead box subgroup O-3a signaling. Cell Physiol Biochem 2015; 35: 1643-53.

[32] Li H, Xu L, Zhao L, Ma Y, Zhu Z, Liu Y, Qu X. Insulin-like growth factor-I induces epithelial to mesenchymal transition via GSK-3β and ZEB2 in the BGC-823 gastric cancer cell line. Oncol Lett 2015; 9: 143-148.

[33] Graham TR, Zhau HE, Odero-Marah VA, Osunkoya AO, Kimbro KS, Tighiouart M, Liu T, Simons JW, O'Regan RM. Insulin-like growth factor-I-dependent up-regulation of ZEB1 drives epithelial-to-mesenchymal transition in human prostate cancer cells. Cancer Res 2008; 68: 2479-88.

[34] Walsh LA, Damjanovski S. IGF-1 increases invasive potential of MCF 7 breast cancer cells and induces activation of latent TGF-β1 resulting in epithelial to mesenchymal transition. Cell Commun Signal 2011; 9: 10.

[35] Wang R, Li H, Guo X, Wang Z, Liang S, Dang C. IGF-I induces epithelial-to-mesenchymal transition via the IGF-IR-Src-MicroRNA-30a-E-cadherin pathway in nasopharyngeal carcinoma cells. Oncol Res 2016; 24: 225-31.

[36] Zhou N, Lu F, Liu C, Xu K, Huang J, Yu D, Bi L. IL-8 induces the epithelial-mesenchymal transition of renal cell carcinoma cells through the activation of AKT signaling. Oncol Lett 2016; 12: 1915-1920.

[37] Ge D, Jing Q, Zhao W, Yue H, Su L, Zhang S, Zhao J. Finding ATF4/p75NTR/IL-8 signal pathway in endothelial-mesenchymal transition by safrole oxide. PLoS One 2014; 9: e99378.

[38] Good RB, Gilbane AJ, Trinder SL, Denton CP, Coghlan G, Abraham DJ, Holmes AM. Endothelial to mesenchymal transition contributes to endothelial dysfunction in pulmonary arterial hypertension. Am J Pathol 2015; 185: 1850-8.

[39] Jia S, Qu T, Wang X, Feng M, Yang Y, Feng X, Ma R, Li W, Hu Y, Feng Y, Ji K, Li Z, Jiang W, Ji J. KIAA1199 promotes migration and invasion by Wnt/β-catenin pathway and MMPs mediated EMT progression and serves as a poor prognosis marker in gastric cancer. PLoS One 2017; 12: e0175058.

[40] Osta WA, Chen Y, Mikhitarian K, Mitas M, Salem M, Hannun YA, Cole DJ, Gillanders WE. EpCAM is overexpressed in breast cancer and is a potential target for breast cancer gene therapy. Cancer Res 2004; 64: 5818-5824.

[41] Noseda M, McLean G, Niessen K, Chang L, Pollet I, Montpetit R, Shahidi R, Dorovini-Zis K, Li L, Beckstead B, Durand RE, Hoodless PA, Karsan A. Notch activation results in phenotypic and functional changes consistent with endothelial-to-mesenchymal transformation. Circ Res 2004; 94: 910-917.

[42] Lee WJ, Park JH, Shin JU, Noh H, Lew H, Yang WI, Yun CO, Lee KH, Lee JH. Endothelial-to-mesenchymal transition induced by Wnt 3a in Keloid pathogenesis. Wound Repair Regen 2015; 23: 435-42.

[43] Wang SH, Chang JS, Hsiao JR, Yen YC, Jiang SS, Liu SH, Chen YL, Shen YY, Chang JY, Chen YW. Tumour cell-derived WNT5B modulates in vitro lymphangiogenesis via induction of partial endothelial-mesenchymal transition of lymphatic endothelial cells. Oncogene 2017; 36: 1503-1515.

[44] Albanese I, Yu B, Al-Kindi H, Barratt B, Ott L, Al-Refai M, de Varennes B, Shum-Tim D, Cerruti M, Gourgas O, Rhéaume E, Tardif JC, Schwertani A. Role of noncanonical wnt signaling pathway in human aortic valve calcification. Arterioscler Thromb Vasc Biol 2017; 37: 543-552.